

Ryerson University
Faculty of Engineering and Architectural Science
Department of Aerospace Engineering

Design and Analysis of a Rocket-Deployed Flying-Wing UAV

Yukei Oyama

AER 870

Aerospace Undergraduate Engineering Thesis

Faculty Advisor – Dr. Chung

April 16, 2021

Abstract

This undergraduate paper demonstrates the design, analysis, and manufacturing of a rocket deployable electric powered experimental unmanned aerial vehicle. The design process begins with defining the volume and dimensions of the allocated payload space for the UAV in the rocket. These dimensions are given by the aerostructures sub team in the Ryerson Rocketry Club. The dimensions given were used to determine the best configuration for the mission. The wing loading, power loading and endurance of the UAV are obtained from the constrained payload volume in the rocket and the avionics system of the of the UAV. The wing area, UAV weight and power requirements were calculated based on the previously determined values. The power requirement determines the motor size and propeller configuration. Aerodynamics, stability, and control were based the selected airfoil and obtained wing area. After completing the design, foam, additive manufacturing, and composite layups were used to create prototypes of the UAV. These prototypes were used to iterate the aircraft and address any immediate changes. The chosen design is a foldable flying wing, once deployed from the rocket has a wingspan of 70 inches, an aspect ratio of 13.35 and a surface area of 367 in². A prototype was created to prove the design feasibility of the UAV. The prototype proved to function as planned, capable of gliding, powered flight, and takeoff.

Acknowledgment

The author would like to thank Dr. Joon Chung for the support and opportunity to create this undergraduate thesis. The Author would also like to thank the Ryerson Rocketry Club and its Captain Alexander Chang for the funding and opportunity to design and manufacture the experimental UAV. Lastly the author would like to thank Ryerson University for the valuable experience gained throughout the undergraduate program.

Table of Contents

Chapter 1: Introduction	1
1.1 Background	1
Chapter 2: Conceptual Design	2
2.1 Design Philosophy	2
2.2 Design Methodology	3
2.3 Design Constraints	5
2.4 Design Choice	5
2.5 Design Specifications.....	8
Chapter 3: Weight Estimation and Material Selection.....	9
3.1 Structural Elements	9
3.1.1 Wing.....	9
3.1.2 Hinge Joint	11
3.1.3 Main hub	12
3.1.4 Control Surfaces - Elevons.....	13
3.2 Electronic Elements	14
3.2.1 Powerplant	14
3.2.2 Battery	14
Chapter 4: Stability and Control, Aerodynamics	15
4.1 Stability and Control	15
4.1.1 Longitudinal Stability/Pitch & Lateral Stability/Roll	15
4.1.2 Directional Stability/Yaw.....	16
4.1.3 General Stability.....	16
4.2 Aerodynamics	17
4.2.1 Airfoil.....	17
4.2.2 Non-Dimensional parameters.....	19
Chapter 5: Deployment and Hinge Mechanisms.....	23

5.1 Hinge Mechanism	23
5.1.1 Section A	25
5.1.2 Section B	26
5.1.3 Section C	27
5.2 Deployment Bay	28
Chapter 6: Manufacturing and Testing	30
6.1 Wing.....	30
6.2 Hinge Mechanism	31
6.2.1 Section A.....	31
6.2.2 Section B	31
6.2.3 Section C	32
6.3 Main Hub	33
Chapter 7: Results	34
Chapter 8: Conclusion.....	35
References	36

List of Figures

Figure 1: UAV Design Methodology.....	3
Figure 2: Conventional Configuration Isometric render	6
Figure 3: Conventional Configuration Front render	6
Figure 4: Flying Wing Isometric render.....	7
Figure 5: Flying Wing Front render	7
Figure 6: Wing Planform	8
Figure 7: Cranked and ESDU Wing MAC	17
Figure 8: MH 70 Orientation One.....	18
Figure 9: MH 70 Orientation Two	19
Figure 10: XFLR5 3D model	20
Figure 11: XFLR5 Lift Distribution.....	20
Figure 12:XFLR5 Moment Reference Location	20
Figure 13: XFLR5 Cl vs Cd graph.....	21
Figure 14: XFLR5 Coefficient of Lift vs AoA graph	21
Figure 15: XFLR5 Coefficient of Moment vs AoA.....	22
Figure 16: XFLR5 Coefficient of Lift/Drag vs AoA	22
Figure 17: Hinge cad blended into the wing	23
Figure 18: Hinge safety factor.....	24
Figure 19: CATIA model of Hinge A	25
Figure 20: CATIA model of Hinge B	26
Figure 21: CATIA model of Hinge C Top Isometric View	27
Figure 22: CATIA model of Hinge C Bottom Isometric View.....	28
Figure 23: Complete Deployment Bay	29
Figure 24: Ejection Bay	29
Figure 25: Flying Wing Prototype	30
Figure 26: Section A Hinge mechanism prototype	31
Figure 27: Section B Hinge mechanism prototype	31
Figure 28: Section C Hinge mechanism prototype	32
Figure 29: Main Hub Prototype	33
Figure 30: Constructed wing prototype.....	34

List of Tables

Table 1: Payload constraints	5
Table 2: Design Configuration Dimensions.....	8
Table 3: Wing Design Matrix	9
Table 4: Wing Weight.....	10
Table 5: Hinge Joint Design Matrix.....	11
Table 6: Hinge Weight Summary	11
Table 7: Main Hub Design Matrix	12
Table 8: Main Hub Weight Summary	12
Table 9: Elevon Design Matrix	13
Table 10: Elevon Weight Summary	13
Table 11: Motor Specifications [1]	14
Table 12: Battery Specification [2]	14
Table 13: Elevon specifications	15
Table 14: ESDU Wing Specifications.....	17
Table 15: Airfoil selection [4].....	18
Table 16: Aerodynamic Coefficient.....	19
Table 17: Axle A Specification.....	25
Table 18: Hinge A Torsion Spring Trade Study	25
Table 19: Magnet A Specification	26
Table 20: Axle B Specification	26
Table 21: Hinge B Torsion Spring Trade Study	27
Table 22: Magnet B Specifications	27
Table 23: Axle C dimensions.....	28
Table 24: Torsion Spring C specifications.....	28

Nomenclature

CAD – Computer Aided Design

MAC - Mean Aerodynamic Chord

RRC – Ryerson Rocketry Club

UAV – Unmanned Aerial Vehicle

Chapter 1: Introduction

1.1 Background

The Ryerson Rocketry Club has decided to implement a UAV as the 2019-2021 payload. This payload will be integrated and deployed from the nosecone of the 30000 ft rocket. The rocket will be launched in New Mexico under the Spaceport competition, where it will be graded and competed for under the payload category. In the previous years, the RRC payload has been comprised of standalone experiments such as the magnetic dampener. The deployed UAV payload will be used to survey the land and assist the recovery team to locate the rocket. This was the first time in RRC history where a payload will be deployed from the rocket.

Chapter 2: Conceptual Design

2.1 Design Philosophy

The design philosophy behind the UAV does not follow conventional methodology due to the high-level compactness and strategic locations of specific components. The UAV designed for this rocket must be aerodynamic, high endurance and robust. The UAV must be designed to survive the launch and ejection from the rocket. These design factors motivate the aircraft to possess a high aspect ratio wing, a propeller powered powerplant and robust mechanisms upon deployment. The UAV must be able to stabilize itself upon deployment and mechanisms must be designed with additional safety margins.

2.2 Design Methodology

The UAV was designed with a unique methodology due to the extreme volumetric constraints and nature of the project. The design methodology is shown in Figure 1.

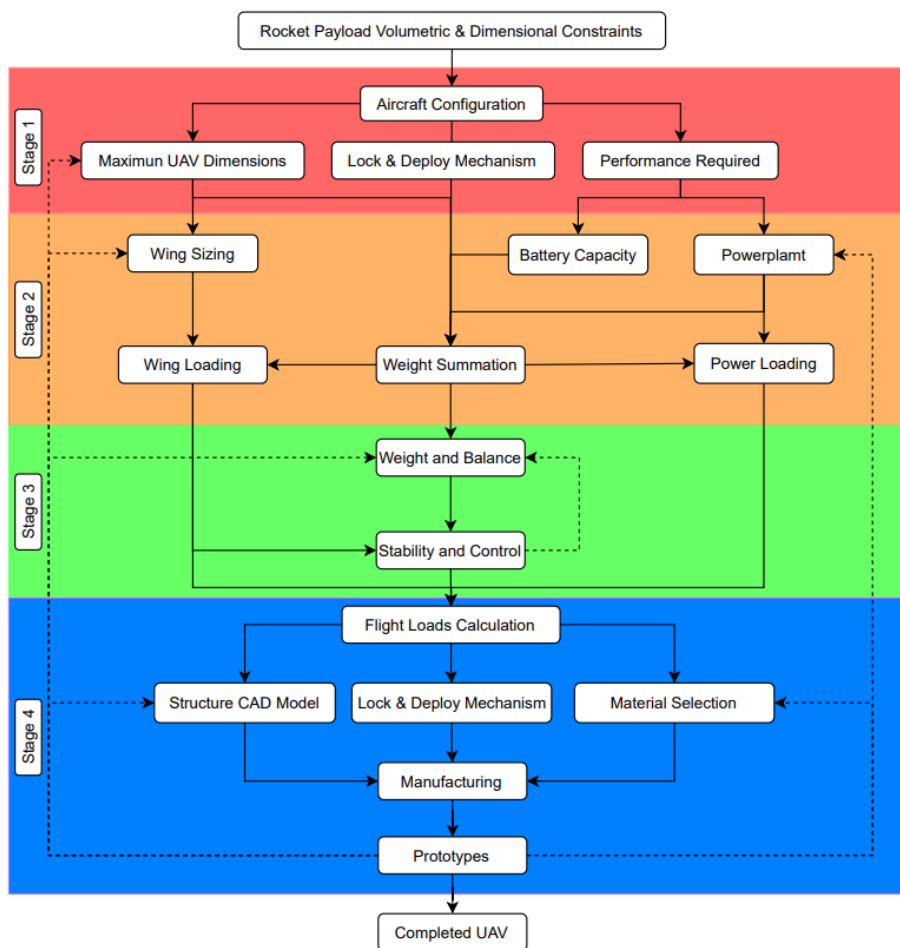


Figure 1: UAV Design Methodology

The first stage in the design methodology is to design a high-level concept and determine the feasibility of the configuration. Stage one starts with the volumetric and dimensional constraints of the fixed payload volume given by RRC. These constraints drive the overall configuration of the UAV. Once the configuration has been finalised maximum UAV dimensions, the mechanism and required performance will be determined based on the volumetric and dimensional constraints of the rocket payload.

The second stage determines the wing and power loading of the UAV. Stage 2 began with the wing sizing derived from the maximum UAV dimensions. The battery capacity and powerplant were derived from the performance required. The weight of the UAV was estimated through the size of the wing, the initial dimensions derived from stage one, the required powerplant to maintain flight and the battery required to power the electronics.

The third stage conducted a weight & balance and to determine the static & dynamic stability of the UAV. The weight & balance will be conducted throughout the design process to ensure static stability of the UAV. The dynamic stability will be used to ensure the aircraft will be able recover upon deployment.

The fourth stage calculated the flight loads, CAD models and prototyping. The flight loads are derived from the flight conditions and used to create safety margins for the structure model and mechanisms. Based on the loads calculated a trade study of materials will be conducted to ensure the UAV will survive not only maneuvers but deployment.

Upon the completion of the four stages, iteration of the design will begin or be completed throughout the methodology.

2.3 Design Constraints

The payload design constraints are as follows:

Table 1: Payload constraints

Maximum Payload Length	5.5 in
Maximum Payload Diameter	12.5 in
Maximum Payload Weight	8.8 lbs

2.4 Design Choice

The three configurations chosen from the constrained payload dimensions are conventional, delta, and flying wing. The mentioned configurations must be highly compact and complex mechanisms would be used to deploy the UAV in a flyable condition from the rocket. Upon the chosen 3, the conventional and flying wing configurations were determined to have the best potential. Both configurations were taken to stage 2 of the design methodology and preliminary CAD models were created. The CAD models were used to determine the specific locations of components and predict the approximate weight of the UAV. Figures 2 and 3 show the conventional configuration. Figures 4 & 5 show the flying wing configuration.

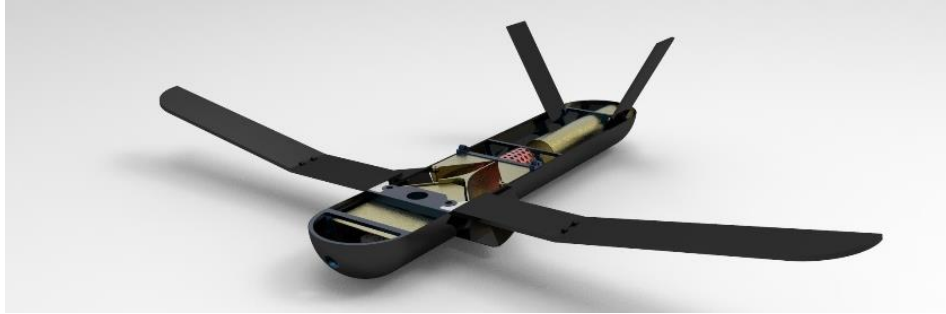


Figure 2: Conventional Configuration Isometric render



Figure 3: Conventional Configuration Front render

The conventional configuration consists of torsion spring loaded wings folding and rotating from the body. The body of the UAV folds into itself with its two halves held together by a lock mechanism. The V tail is popped into place with torsion springs once the body of the UAV has been successfully deployed. The propulsion mechanism is a EDF motor with intakes extruding out as the body unfolds. This configuration allows for a high aspect ratio wing and minimal mechanisms increasing reliability while deploying from the rocket. However, this configuration limits the surface area of the wing thus increasing the airspeed to maintain steady level flight. The EDF motor also consumes large amounts of power from the battery thus non suitable for a high endurance mission.



Figure 4: Flying Wing Isometric render



Figure 5: Flying Wing Front render

The flying wing configuration consists of torsion springs unfolding at each section of the wing. This compact method allows the UAV to be highly portable without compromising structure and wing sizing. This configuration allows for a high aspect ratio wing while maintaining a respectable wing area. The wing area allows the aircraft to fly at slower speeds thus increasing the endurance of the aircraft. However, the numerous mechanisms required to unfold the aircraft increases complexity and risk of failure. The flying wing satisfies the design philosophy and complex mechanisms were designed with a safety margin to increase reliability. Thus, the flying wing was chosen as the final configuration.

2.5 Design Specifications

Once the design configuration has been reached, possible dimensions have been calculated and determined based on the payload constraints. These dimensions were iterated based on the location of systems, control surfaces and powerplant location. These dimensions were modeled and shown in the planform view. These dimensions are tabulated in Table 2.

Table 2: Design Configuration Dimensions

<u>Dimension</u>	<u>Inboard</u>	<u>Midboard</u>	<u>Outboard</u>
Span (in)	11.75	12.35	10.95
Chord (in)	5.40	5.02	5.35
Sweep (deg)	10	10	30
Dihedral (deg)	0	2.5	5
Taper Ratio	1		
Aspect Ratio	13.35		
Surface Area (in ²)	367		
Total Span (in)	70		

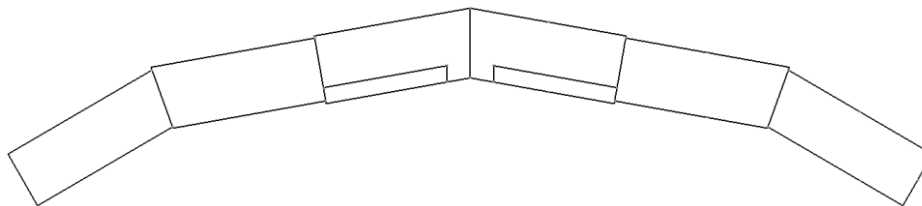


Figure 6: Wing Planform

Chapter 3: Weight Estimation and Material Selection

3.1 Structural Elements

3.1.1 Wing

The wing of the aircraft must be structurally rigid, light weight and be able to survive the launch acceleration of the rocket. In order to satisfy these conditions a design matrix was used to determine the optimal material. The design matrix compares the following factors, strength, manufacturability, cost, and weight to determine the best material. The materials are sorted into three categories, the core, spar and skin. These three materials are combined to create the wing and will be weighed against the combinations shown in the design matrix in Table 3.

Table 3: Wing Design Matrix

Core	Spar	Skin	Strength	Manufacturability	Cost	Weight
Foam	Carbon Fiber	Fiber Glass	5	5	5	5
3D Print	Carbon Fiber	Monokote Sheet	5	5	5	3
Ply Ribs	Carbon Fiber	Monokote Sheet	3	4	4	5

The design matrix shows that the combination of a foam core, carbon fiber spar and fiber glass skin satisfy all four parameters and meet the requirements.

The weight of each individual part was calculated and tabulated in Table 4. The weight of the foam core was calculated using the density of the foam and the volume of the wing obtained from the CATIA model. The weight of the carbon spar was calculated using the density of the carbon fiber rod and the required spar length obtained from the CATIA model. The weight of the fiberglass skin was calculated using the density of the fiberglass, epoxy ratio, and the required surface area obtained from the CATIA model.

Table 4: Wing Weight

	Inboard	Midboard	Outboard
Foam Core (lb)	0.00878	0.00742	0.00657
Carbon Fiber Spar (lb)	0.00095	0.00095	0.00095
Fiberglass Skin (lb)	0.00623	0.00572	0.00538

3.1.2 Hinge Joint

The hinge of the aircraft is responsible for the deployment of the wings and is a key aspect in the compactness of the design. The hinge must be designed for the twisting and bending caused by aerodynamic forces, light weight, cost effective and reusable. A design matrix was used to determine the optimal material required for the aircraft as in Table 5. The hinge mechanism is comprised of two parts, the hinge and axle. The two parts were combined to create the hinge mechanism and weighed against each other to determine the optimal material required for the hinge.

Table 5: Hinge Joint Design Matrix

Hinge	Axle	Strength	Manufacturability	Cost	Weight
3D Print	Carbon Fiber	4	<u>5</u>	<u>5</u>	<u>5</u>
Aluminum	Carbon Fiber	<u>5</u>	3	2	3

The weight of each individual component was calculated and tabulated in Table 6. The 3D printed hinge was modelled in CATIA and exported into a slicer software to determine the estimated weight. The axle weight was determined from the required length of the axle.

Table 6: Hinge Weight Summary

	Inboard	Midboard	Outboard
3D Print Hinge (lb)	0.05	0.018	0.0078
Carbon Fiber Axle (lb)	0.005	0.005	0.005

3.1.3 Main hub

The main hub of the aircraft is a central piece in the assembly of other components such as the avionics, powerplant, and the inboard section hinges. The main hub must be designed for the attached powerplant, and modular surface to mount the avionics. A design matrix was used to determine the optimal material as shown in Table 7.

Table 7: Main Hub Design Matrix

Hub	Nacelle	Strength	Manufacturability	Cost	Weight
3D Print	Fiber Glass	4	<u>5</u>	<u>5</u>	<u>5</u>
Aluminum	Fiber Glass	<u>5</u>	3	2	3

The weight of each individual component was calculated and tabulated in Table 8. The 3D printed main hub was modelled in CATIA and exported into a slicer software to determine the estimated weight. The nacelle was modelled in CATIA and the volume as used to determine the weight.

Table 8: Main Hub Weight Summary

	Main Hub
3D Print Hub (lb)	0.057
Fiber Glass Nacelle (lb)	0.025

3.1.4 Control Surfaces - Elevons

The elevons act as control surfaces required to maneuver the flying wing. The elevons must be designed for the aerodynamic loads endured during maneuvers and provide a reflex for stability & control. A design matrix was used to determine the optimal material as shown in Table 9.

Table 9: Elevon Design Matrix

Elevon	Strength	Manufacturability	Cost	Weight
Balsa Edge	4	<u>5</u>	<u>5</u>	<u>5</u>
3D Print	<u>5</u>	3	2	2
Foam	<u>3</u>	2	5	5

The weight of the elevon was determined through the analysis of existing balsa trailing edge and tabulated in Table 10.

Table 10: Elevon Weight Summary

	Elevon
Balsa Trailing Edge (lb)	0.012

3.2 Electronic Elements

3.2.1 Powerplant

The powerplant was chosen on many factors, including size, power, and weight. The final powerplant selected is the RS 1606 4000KV motor. Table 11 shows the specifications of the motor.

Table 11: Motor Specifications [1]

Motor	RS 1606 4000KV
25% Power (HP)	0.061
50% Power (HP)	0.155
100% Power (HP)	0.76
Propeller	HQ 4x4.3x3
Motor weight (lb)	0.0348
Recommended battery voltage	3 cell / 4 cell
Max Thrust (lb)	2.26

3.2.2 Battery

The battery was selected based on the recommended number of cells from the motor manufacturer website, and estimated mission time. Table 12 shows the battery specifications.

Table 12: Battery Specification [2]

LiPo Battery	Tattu
Voltage (V)	14.2
Capacity (Mah)	1300
Weight (lb)	0.33
Dimensions (in)	2.846 x 1.402 x 1.17

Chapter 4: Stability and Control, Aerodynamics

4.1 Stability and Control

4.1.1 Longitudinal Stability/Pitch & Lateral Stability/Roll

Conventional aircraft use an aileron and horizontal stabilizer to achieve stability and movement. An aileron gives the aircraft lateral stability and roll control where the horizontal stabilizer provides longitudinal stability and pitch control.

However, on a flying wing these control surfaces do not exist. To assure the aircraft is stable, compromises must be made to achieve steady flight.

An elevon was implemented in the inboard section of the flying to control the aircraft's pitch and roll. The elevon will also be responsible for the longitudinal and lateral stability of the aircraft. Table 13 shows the specifications of the elevon.

Table 13: Elevon specifications

Elevon Width (in)	1.5
Elevon Length (in)	11
Elevon Area (in ²)	16.5

4.1.2 Directional Stability/Yaw

Conventional aircraft use a vertical stabilizer to achieve directional stability and yaw. The flying wing does not have this capability thus rely on the leading-edge sweep of the aircraft to maintain directional stability. This aircraft has a ESDU sweep of approximately 13 degrees.

4.1.3 General Stability

The static margin of the aircraft dictates its manoeuvrability and stability characteristics. The neutral point of the aircraft is important since it determines the location of the CG based on a static margin. The neutral point was calculated using a neutral point calculator [3]. Since the flying wing does not have an empennage, the neutral point is located at the aerodynamic center of the wing. Thus, the MAC of the wing must be calculated, to determine the neutral point of the aircraft. The MAC of a conventional tapered wing is easily determined through geometry or calculations. The calculation of a MAC of a compound swept wing is highly complex, thus requiring an ESDU wing to relate it to. The center of gravity of the aircraft was ensured to have a static margin of 15%.

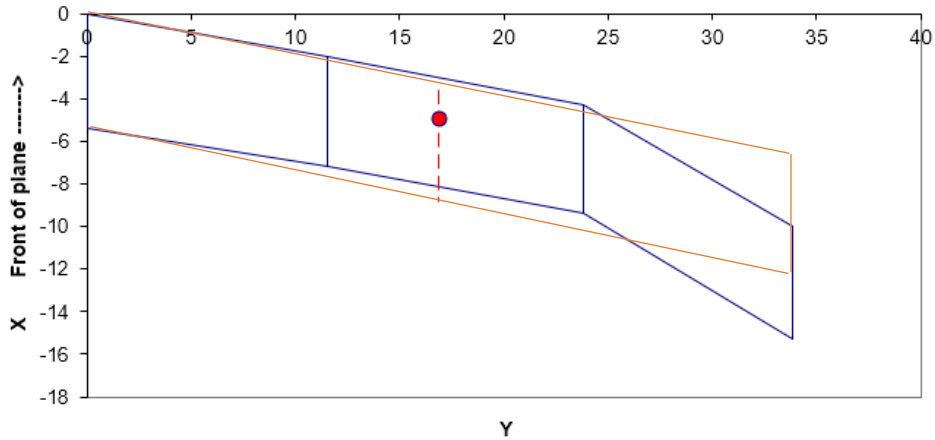


Figure 7: Cranked and ESDU Wing MAC

Table 14: ESDU Wing Specifications

ESDU Surface Area (in ²)	360
ESDU Root (in)	5.4
ESDU Tip (in)	5.35
MAC (in)	5.18
Neutral Point (from leading edge) (in)	4.92
0.25 Sweep	15.95
CG Location (from leading edge) (in)	4.25

4.2 Aerodynamics

4.2.1 Airfoil

Conventional aircraft has a horizontal tail to not only provide lateral stability but also counter act the lift force of wing acting around the center of gravity. This is achieved by the horizontal tail creating a downforce during flight.

In order to compensate for the lack of a horizontal stabilizer on the flying wing, an airfoil with a reflex was chosen. The airfoil must also possess a

moment coefficient as close to as 0, to ensure that the aircraft can correct itself. Table 15 shows the airfoils selected for a trade study. The MH series proved to be the most popular and reliable, thus was chosen for the final selection. The airfoil chosen must not only be aerodynamically efficient but adhere to the physical constraints of the rocket once folded. Thus, the MH 70 was chosen as the final airfoil. Figure 8&9 shows a top view of two orientations of the theoretical fit of the MH 70 airfoil in its folded stage constrained in the rocket tube.

Table 15: Airfoil selection [4]

Airfoil	Max Cl/Cd	Cm	Cl Max	Cl min	t/c
MH 60	84.5	-0.006	1.03	-0.62	10.28
MH 70	84.8	-0.003	1.32	-0.56	11.08
MH 80	85.2	-0.001	1.65	-0.5	12.72
HS 520	84.37	-0.022	1.283	-0.584	9.8
Eppler 344	94	-0.032	1.5	-0.29	14.7
LA2573A	102	0.0117	1.33	-0.52	13.7

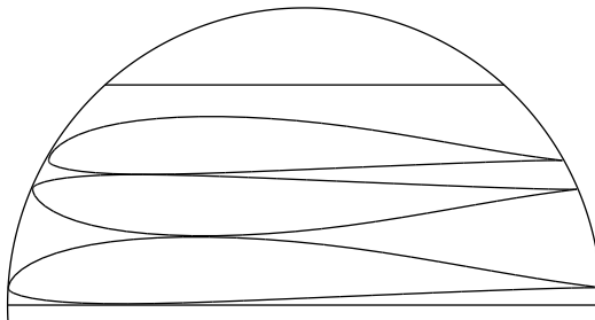


Figure 8: MH 70 Orientation One

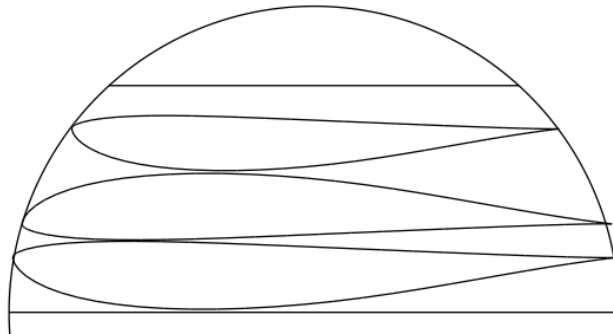


Figure 9: MH 70 Orientation Two

Orientation one was chosen due to the greater connection length between the inboard and midboard airfoil sections. The orientation of the airfoil would also determine the location of the avionics bay. Orientation one would result in the avionics bay being on the top, while orientation two would result in the avionics bay being on the bottom.

4.2.2 Non-Dimensional parameters

XFLR5 was used to determine the aerodynamic coefficients of the aircraft. The results are tabulated in Table 16 and show through Figure 10-16. Figure 10 show the equivalent 3D model of the aircraft.

Table 16: Aerodynamic Coefficient

Parameters	Values
Cruise Speed	32 ft/s
AoA	0 deg
CL	0.303
CD	0.021
Efficiency	0.919
CL/CD	14.654
Cm	-0.088

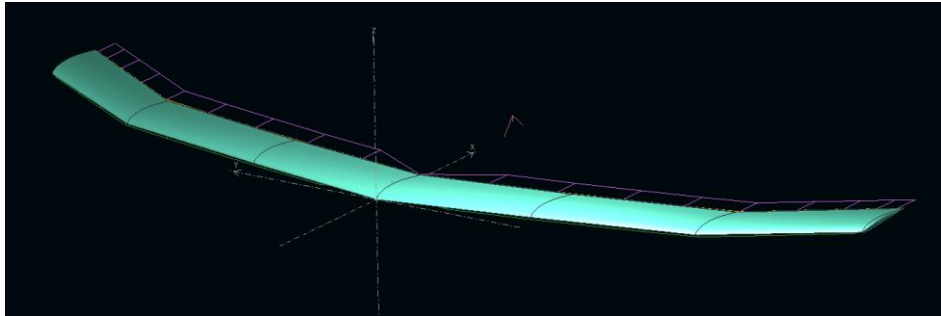


Figure 10: XFLR5 3D model

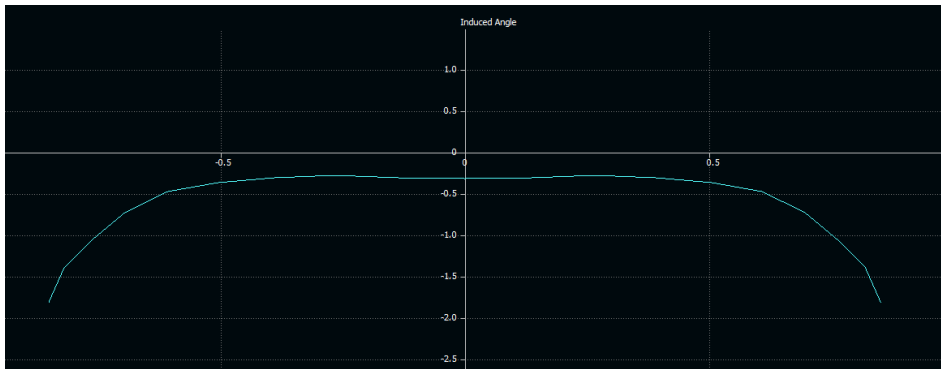


Figure 11: XFLR5 Lift Distribution

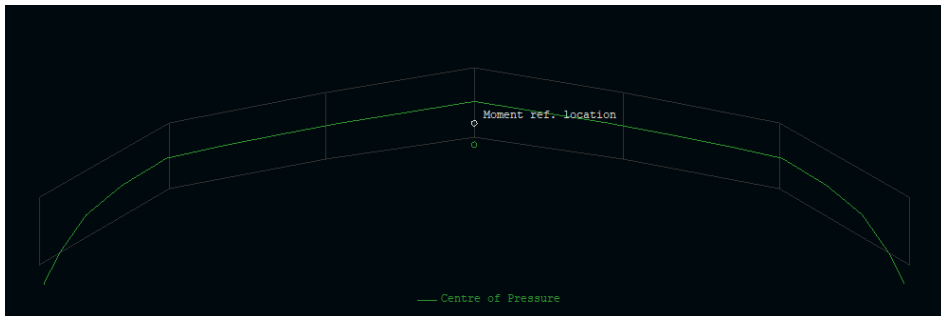


Figure 12: XFLR5 Moment Reference Location

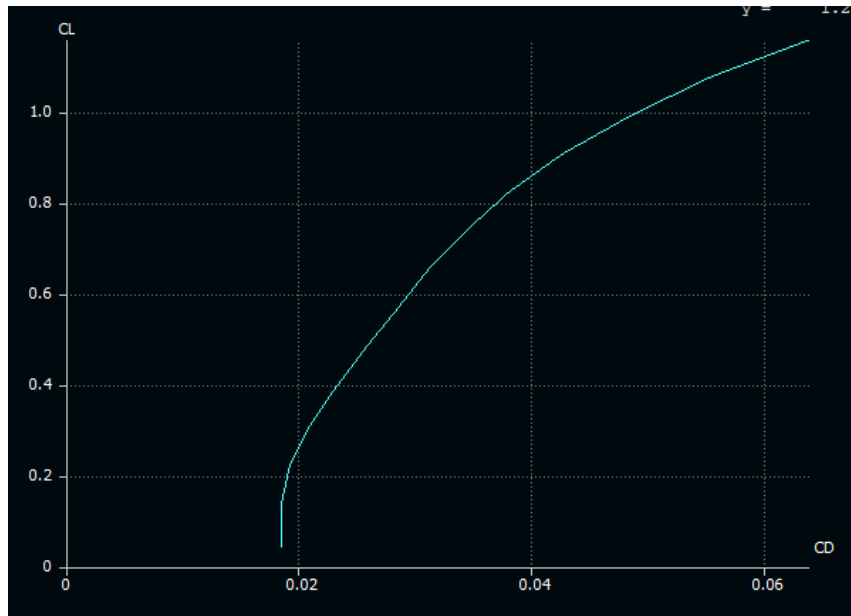


Figure 13: XFLR5 Cl vs Cd graph

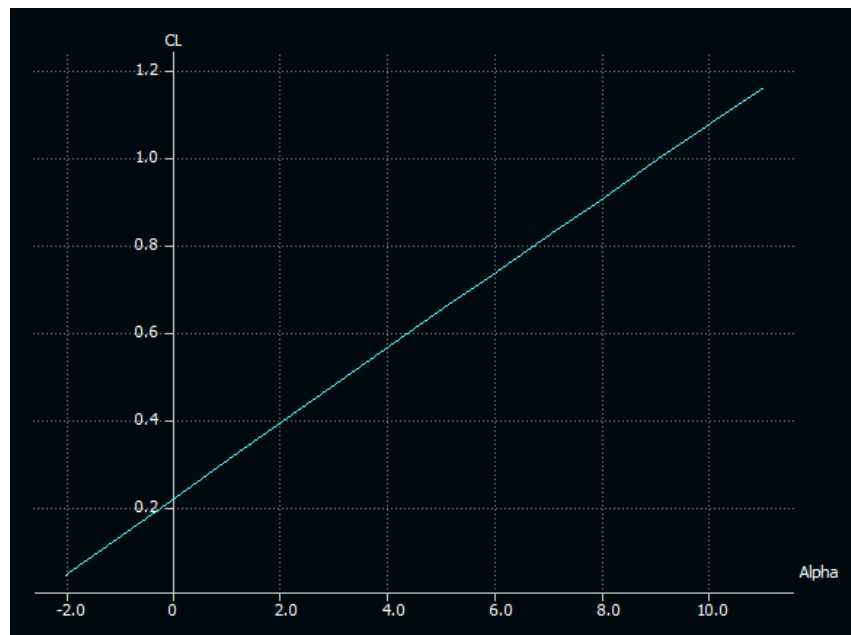


Figure 14: XFLR5 Coefficient of Lift vs AoA graph

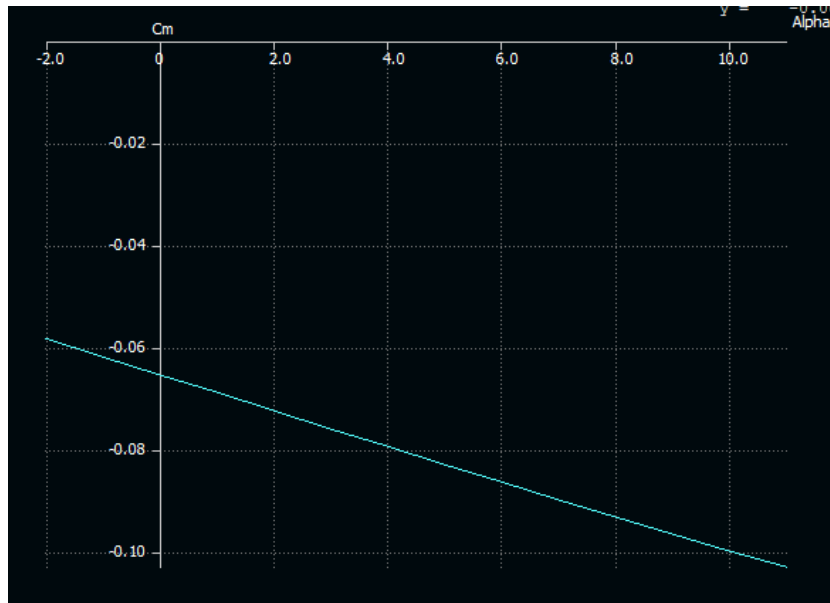


Figure 15: XFLR5 Coefficient of Moment vs AoA

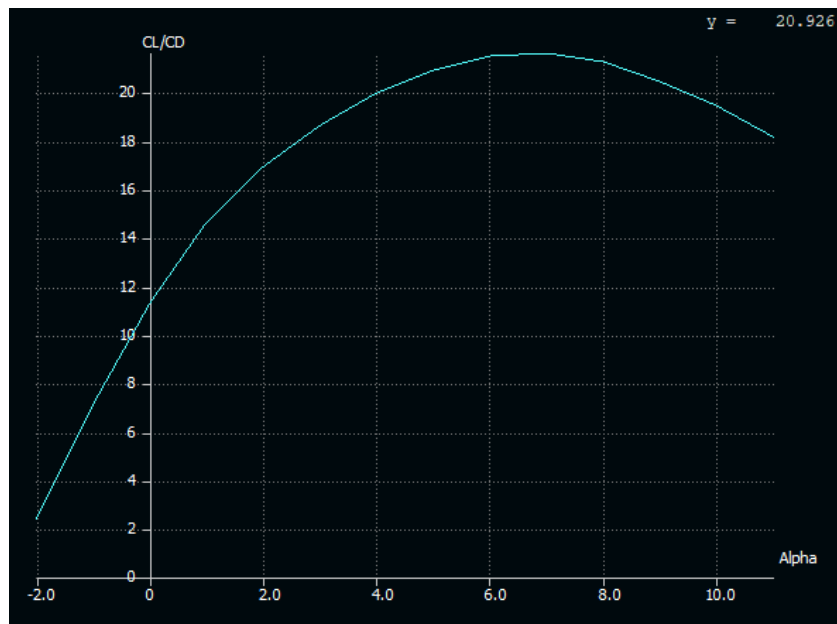


Figure 16: XFLR5 Coefficient of Lift/Drag vs AoA

Chapter 5: Deployment and Hinge Mechanisms

5.1 Hinge Mechanism

The hinge mechanism is used to fold the aircraft out in a flyable configuration. The hinges are 3D printed, combined with carbon fiber axles, deployed using steel torsion springs and locked via magnets.

The hinge was designed so that the wing rotates around each other at a tangent to each other. This allows the transition between the hinge and the airfoil to be seamless as seen in Figure 17. Circular holes were created to epoxy and mount the carbon fiber rods, and lightening holes were used to make the hinge as light as possible.

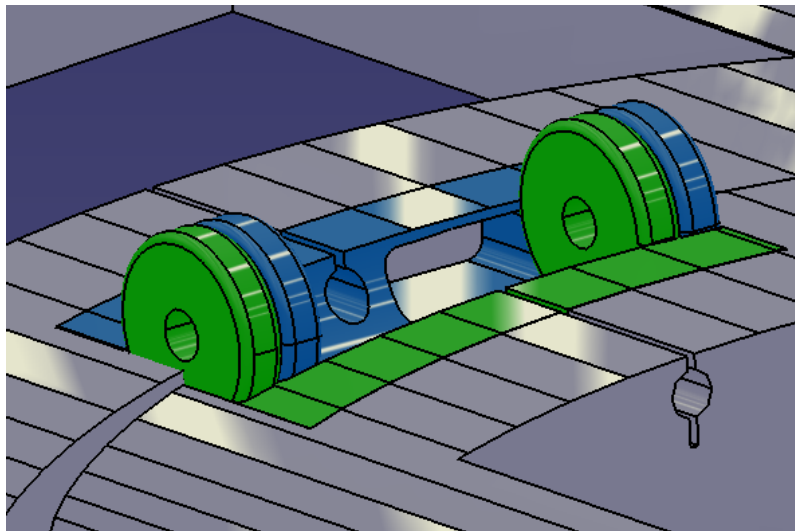


Figure 17: Hinge cad blended into the wing

A carbon fiber rod was used to keep the two 3D printed hinges together. Carbon fiber was used due to its light weight and robust properties.

Torsion springs are categorized by their respective angles and size, thus varying different properties of resistance and strength. Since the hinges would need to rotate 180 degrees, a trade study was conducted to determine the best type of torsion spring. This was determined through its ability to lift the weight of each respective section, size, and safety factor. The safety factor was derived from the datum where the spring would have completed the deployment. The safety factor reflects how much force the spring has left after it has fully folded out.

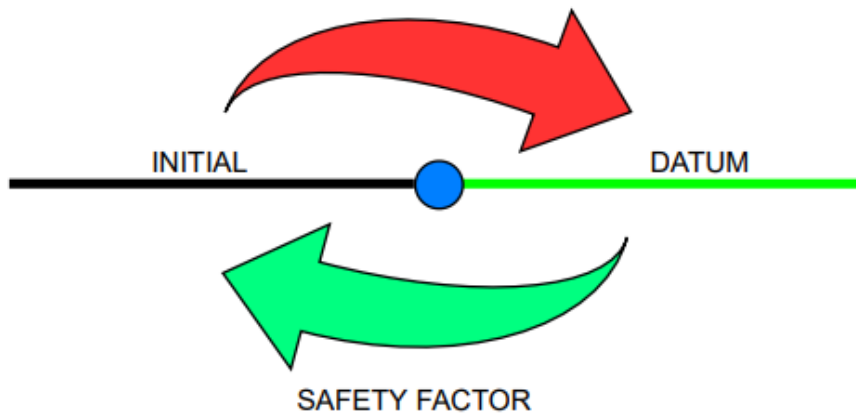


Figure 18: Hinge safety factor

Magnets were used as the locking mechanism due to its passive ability to connect and high degree of reliability. Although it is heavier than a conventional mechanism, due to the scale of the project, reliability was prioritized. The magnet chosen for this project are the N52 magnets, due to its strength and compact size, compared to competitors.

5.1.1 Section A

5.1.1.1 3D Printed Hinge A

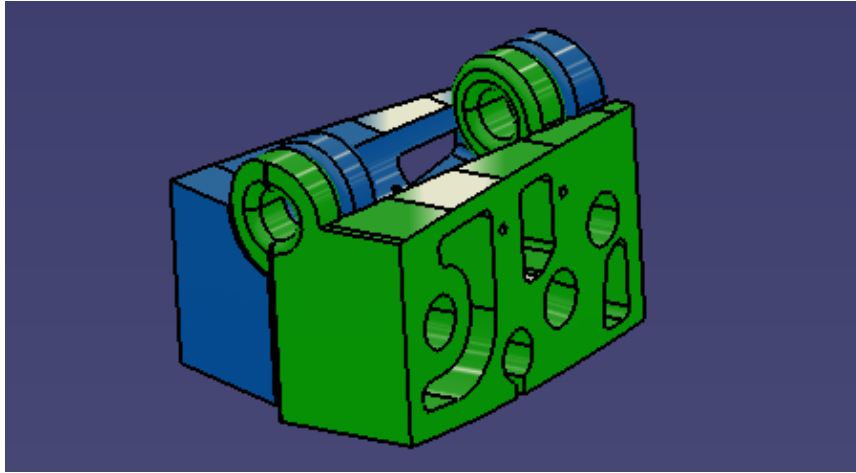


Figure 19: CATIA model of Hinge A

5.1.1.2 Axle A

Table 17: Axle A Specification

Axle Material	Carbon Fiber
Diameter (in)	0.125
Length (in)	1.5

5.1.1.3 Torsion Spring A

Table 18: Hinge A Torsion Spring Trade Study

Spring Angle (in)	Outer Diameter (in)	Shaft Diameter (in)	Spring Length at Max torque (in)	Max Moment (lb in)	Safety Factor (from datum)
225	0.366	0.24	0.268	0.56	143%
270	0.29	0.21	0.291	0.5	261%
315	0.359	0.24	0.271	0.33	207%
360	0.271	0.187	0.242	0.234	154%

5.1.1.4 Magnets A

Table 19: Magnet A Specification

Magnet Type	N52
Diameter (in)	0.25
Length (in)	0.25
Attraction Force (lb)	5.13

5.1.2 Section B

5.1.2.1 3D Printed Hinge B

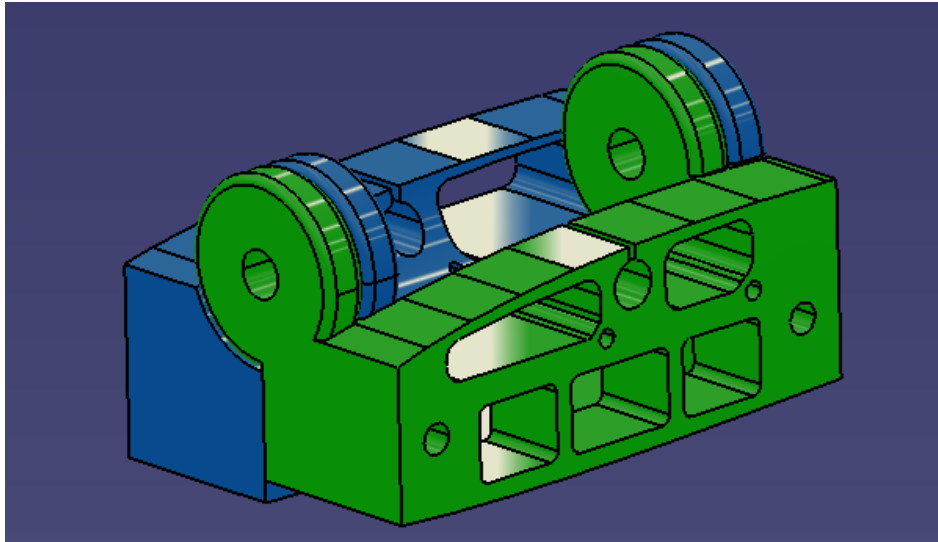


Figure 20: CATIA model of Hinge B

5.1.2.2 Axle B

Table 20: Axle B Specification

Axle Material	Carbon Fiber
Diameter (in)	0.25
Length (in)	2

5.1.2.3 Torsion Spring B

Table 21: Hinge B Torsion Spring Trade Study

Spring Angle (in)	Outer Diameter (in)	Shaft Diameter (in)	Spring Length at Max torque (in)	Max Moment (lb in)	Safety Factor (from datum)
225	0.578	0.36	0.789	4.9	150%
270	0.556	0.359	0.415	2.14	82%
315	0.47	0.3	0.659	1.9	108%
360	0.508	0.343	0.47	1.5	91%

5.1.1.4 Magnets B

Table 22: Magnet B Specifications

Magnet Type	N52
Height (in)	0.25
Width (in)	0.25
Length (in)	1
Attraction Force (lbs)	18

5.1.3 Section C

5.1.3.1 3D Printed Hinge C

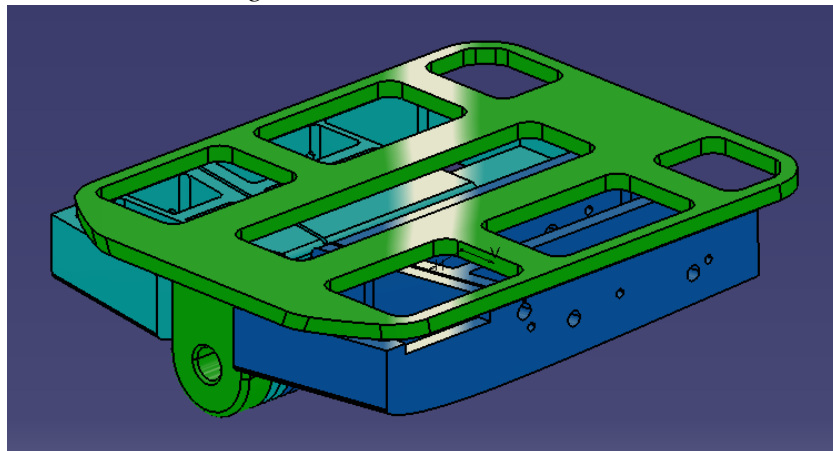


Figure 21: CATIA model of Hinge C Top Isometric View

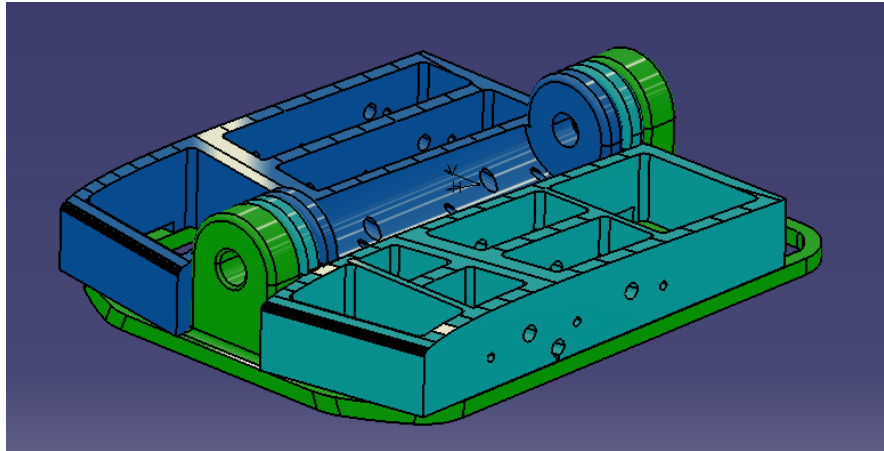


Figure 22: CATIA model of Hinge C Bottom Isometric View

5.1.3.2 Axle C

Table 23: Axle C dimensions

Axle Material	Carbon Fiber
Diameter (in)	0.25
Length (in)	4.75

5.1.3.3 Torsion Spring C

Table 24: Torsion Spring C specifications

Spring Angle (in)	Outer Diameter (in)	Shaft Diameter (in)	Spring Length at Max torque (in)	Max Moment (lb in)	Safety Factor (from datum)
225	0.936	0.6	1.158	14	150%
270	0.784	0.52	0.727	5.1	49%
315	0.763	0.48	1.461	10	108%
360	0.798	0.516	0.82	5.52	63%

5.2 Deployment Bay

The deployment bay is comprised of two parts, the main structural bay and ejection bay. The structural bay will ensure the aircraft will not get crushed

upon deployment from the rocket. The ejection bay will be ejected via the tension of the cord. The cord is connected to the bulk heads on the rocket and pulled via the main chute. Once the deployment bay is ejected from the rocket it will eject the aircraft when the cord is fully taut.

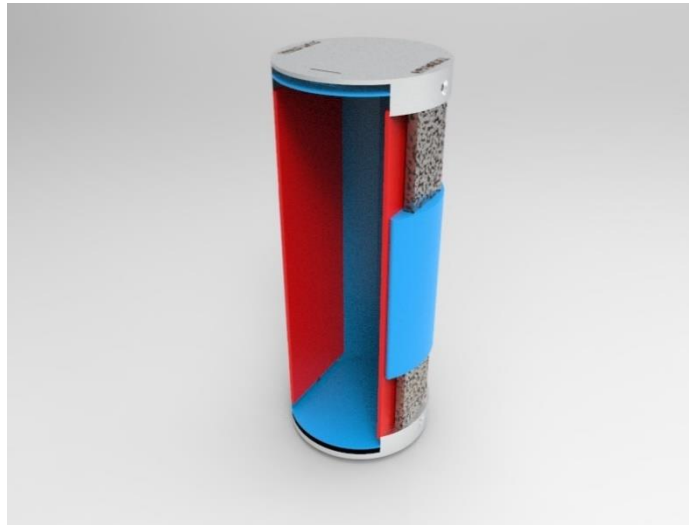


Figure 23: Complete Deployment Bay

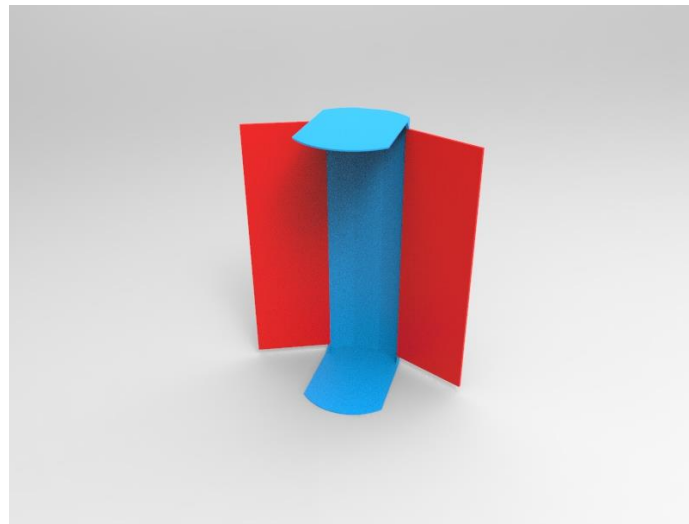


Figure 24: Ejection Bay

Chapter 6: Manufacturing and Testing

6.1 Wing

Figure 25 shows the prototype of the wing. The foam was cut using nichrome wire and encased in fiberglass composite. Carbon fiber were used as the spar. Since this was a prototype to demonstrate flight, the hinges were replaced with connection rods.

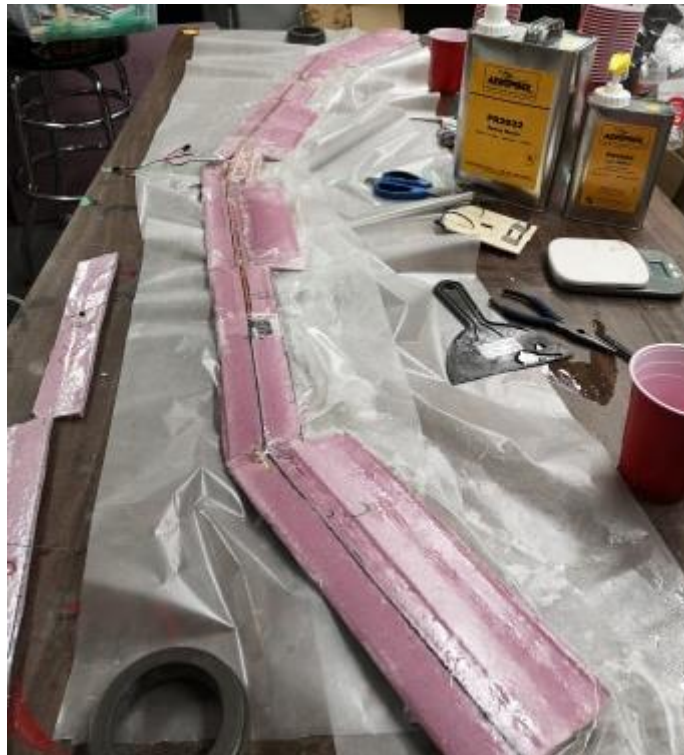


Figure 25: Flying Wing Prototype

6.2 Hinge Mechanism

6.2.1 Section A

Section A connects the outboard and midboard wing of the aircraft together. Section A was created using 3D printing and steel torsion springs. Carbon fiber rods will be used to connect section A to section B.



Figure 26: Section A Hinge mechanism prototype

6.2.2 Section B

Section B connects the inboard and midboard wing of the aircraft together. Section B was created using 3D printing and steel torsion springs. Carbon fiber rods will be used to connect section B to section C.



Figure 27: Section B Hinge mechanism prototype

6.2.3 Section C

Section C connects the two-inboard section of the wing together. Section C was created using 3D printing and steel torsion springs. A bolt was used for this prototype, the final model will have a carbon fiber axel.



Figure 28: Section C Hinge mechanism prototype

6.3 Main Hub

The main hub is responsible for mounting the avionic components and the connection point between the port and starboard side of the aircraft. The main hub was 3D printed and assembled with a bolt. A bolt was used for this prototype, the final model will have a carbon fiber axel. Access ports were created to let the wires into the bays below. The lower bays will house the smaller avionics and components that are not the main board.



Figure 29: Main Hub Prototype

Chapter 7: Results

Before the campus was closed, a prototype was created and flown with prospective results. The prototype proved to be capable of gliding, powered flight, and takeoff. However, during the test, the connection point with the inboard and midboard wing failed, resulting in the prototype to be disintegrated. Figure 30 shows the prototype with myself for scale. For reference I am 5'7.



Figure 30: Constructed wing prototype

Chapter 8: Conclusion

In conclusion, this undergraduate paper demonstrates the design, analysis, and manufacturing of a rocket deployable electric powered experimental unmanned aerial vehicle. The chosen design is a foldable flying wing, once deployed from the rocket has a wingspan of 70 inches, an aspect ratio of 13.35 and a surface area of 367 in². A prototype was created to prove the design feasibility of the UAV. The prototype proved to function as planned, capable of gliding, powered flight, and takeoff. Due to COVID-19 the campus was closed, and the Spaceport competition was cancelled. Thus, the final product was not constructed. As the year progresses and the campus opens once again, the goal of this project will be to complete the UAV. Upon completion the UAV will be tested in competition to validate the design feasibility.

References

- [1] “EMAX RS 1606 Brushless Racing Motor 3300kV/4000kV,” *AirBlade UAV*. [Online]. Available: <https://www.airbladeuav.com/products/emax-rs1606-brushless-racing-motor-3300kv-4000kv>. [Accessed: 16-Apr-2021].
- [2] *Tattu 14.8V 1300mAh LiPo Battery Pack 45C 4S with XT60 Plug for Nemesis 240 Mini Tweaker 180 Micro Quad LRC Freestyle VI MXP180 Danaus Vortex FLIP 250S Mini FLIP RC Heli Airplane Drone FPV Quadcopter, Battery Packs - Amazon Canada*. [Online]. Available: <https://www.amazon.ca/Tattu-Battery-1300mAh-14-8V-Airplane/dp/B013I9RSEU>. [Accessed: 16-Apr-2021].
- [3] “Attachment browser: CGCalc_1.05.zip by Montag DP - RC Groups,” *RC Groups RSS*. [Online]. Available: <https://www.rcgroups.com/forums/attachment.php?attachmentid=6595959>. [Accessed: 16-Apr-2021].
- [4] *Airfoil Tools*. [Online]. Available: <http://airfoiltools.com/>. [Accessed: 16-Apr-2021].

Appendix A

